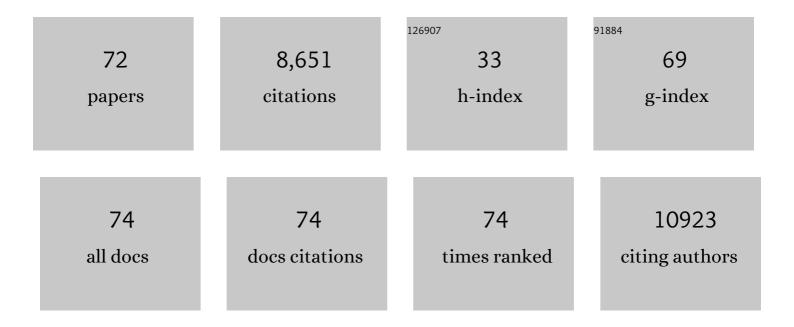
List of Publications by Year in descending order

Source: https://exaly.com/author-pdf/1067836/publications.pdf Version: 2024-02-01



Ρενςεεί ΔΝ

#	Article	IF	CITATIONS
1	Ultrathin metal–organic framework nanosheets for electrocatalytic oxygen evolution. Nature Energy, 2016, 1, .	39.5	1,979
2	General synthesis and definitive structural identification of MN4C4 single-atom catalysts with tunable electrocatalytic activities. Nature Catalysis, 2018, 1, 63-72.	34.4	1,476
3	Structural transformation of highly active metal–organic framework electrocatalysts during the oxygen evolution reaction. Nature Energy, 2020, 5, 881-890.	39.5	647
4	Efficient Visibleâ€Lightâ€Driven Carbon Dioxide Reduction by a Singleâ€Atom Implanted Metal–Organic Framework. Angewandte Chemie - International Edition, 2016, 55, 14310-14314.	13.8	612
5	Dynamic traction of lattice-confined platinum atoms into mesoporous carbon matrix for hydrogen evolution reaction. Science Advances, 2018, 4, eaao6657.	10.3	460
6	Single atom tungsten doped ultrathin α-Ni(OH)2 for enhanced electrocatalytic water oxidation. Nature Communications, 2019, 10, 2149.	12.8	363
7	Atypical Oxygen-Bearing Copper Boosts Ethylene Selectivity toward Electrocatalytic CO ₂ Reduction. Journal of the American Chemical Society, 2020, 142, 11417-11427.	13.7	250
8	Structurally Wellâ€Ðefined Au@Cu _{2â^'} <i>_x</i> S Core–Shell Nanocrystals for Improved Cancer Treatment Based on Enhanced Photothermal Efficiency. Advanced Materials, 2016, 28, 3094-3101.	21.0	228
9	Design of ultrathin Pt-Mo-Ni nanowire catalysts for ethanol electrooxidation. Science Advances, 2017, 3, e1603068.	10.3	224
10	Ni ^{II} Coordination to an Alâ€Based Metal–Organic Framework Made from 2â€Aminoterephthalate for Photocatalytic Overall Water Splitting. Angewandte Chemie - International Edition, 2017, 56, 3036-3040.	13.8	175
11	Efficient Visibleâ€Lightâ€Driven Carbon Dioxide Reduction by a Singleâ€Atom Implanted Metal–Organic Framework. Angewandte Chemie, 2016, 128, 14522-14526.	2.0	174
12	Reordering d Orbital Energies of Single‣ite Catalysts for CO ₂ Electroreduction. Angewandte Chemie - International Edition, 2019, 58, 12711-12716.	13.8	166
13	Unraveling the Interfacial Charge Migration Pathway at the Atomic Level in a Highly Efficient Zâ€Scheme Photocatalyst. Angewandte Chemie - International Edition, 2019, 58, 11329-11334.	13.8	152
14	Colloidal Synthesis of Ultrathin Monoclinic BiVO ₄ Nanosheets for Z-Scheme Overall Water Splitting under Visible Light. ACS Catalysis, 2018, 8, 8649-8658.	11.2	151
15	N-doped Ni-Mo based sulfides for high-efficiency and stable hydrogen evolution reaction. Applied Catalysis B: Environmental, 2020, 276, 119137.	20.2	150
16	The Flexibility of an Amorphous Cobalt Hydroxide Nanomaterial Promotes the Electrocatalysis of Oxygen Evolution Reaction. Small, 2018, 14, e1703514.	10.0	121
17	Delocalized electron effect on single metal sites in ultrathin conjugated microporous polymer nanosheets for boosting CO ₂ cycloaddition. Science Advances, 2020, 6, eaaz4824.	10.3	68
18	Interface engineered <i>in situ</i> anchoring of Co ₉ S ₈ nanoparticles into a multiple doped carbon matrix: highly efficient zinc–air batteries. Nanoscale, 2018, 10, 2649-2657.	5.6	66

#	Article	IF	CITATIONS
19	Feâ€O Clusters Anchored on Nodes of Metal–Organic Frameworks for Direct Methane Oxidation. Angewandte Chemie - International Edition, 2021, 60, 5811-5815.	13.8	66
20	Directed Biofabrication of Nanoparticles through Regulating Extracellular Electron Transfer. Journal of the American Chemical Society, 2017, 139, 12149-12152.	13.7	64
21	Controlled chelation between tannic acid and Fe precursors to obtain N, S co-doped carbon with high density Fe-single atom-nanoclusters for highly efficient oxygen reduction reaction in Zn–air batteries. Journal of Materials Chemistry A, 2020, 8, 17136-17149.	10.3	64
22	Dynamic Restructuring of Coordinatively Unsaturated Copper Paddle Wheel Clusters to Boost Electrochemical CO ₂ Reduction to Hydrocarbons**. Angewandte Chemie - International Edition, 2022, 61, .	13.8	61
23	Selective hydrogenation of unsaturated aldehydes over Pt nanoparticles promoted by the cooperation of steric and electronic effects. Chemical Communications, 2018, 54, 908-911.	4.1	55
24	Manganese deception on graphene and implications in catalysis. Carbon, 2018, 132, 623-631.	10.3	54
25	Breaking Platinum Nanoparticles to Singleâ€Atomic Ptâ€C ₄ Coâ€catalysts for Enhanced Solarâ€toâ€Hydrogen Conversion. Angewandte Chemie - International Edition, 2021, 60, 2541-2547.	13.8	51
26	Covalently anchoring cobalt phthalocyanine on zeolitic imidazolate frameworks for efficient carbon dioxide electroreduction. CrystEngComm, 2020, 22, 1619-1624.	2.6	48
27	Toward a Unified Identification of Ti Location in the MFI Framework of High-Ti-Loaded TS-1: Combined EXAFS, XANES, and DFT Study. Journal of Physical Chemistry C, 2016, 120, 20114-20124.	3.1	45
28	Enhanced CO ₂ electroreduction <i>via</i> interaction of dangling S bonds and Co sites in cobalt phthalocyanine/ZnIn ₂ S ₄ hybrids. Chemical Science, 2019, 10, 1659-1663.	7.4	45
29	Mechanisms on the morphology variation of hematite crystals by Al substitution: The modification of Fe and O reticular densities. Scientific Reports, 2016, 6, 35960.	3.3	43
30	Reordering d Orbital Energies of Single‣ite Catalysts for CO ₂ Electroreduction. Angewandte Chemie, 2019, 131, 12841-12846.	2.0	40
31	Atomically defined Co on two-dimensional TiO2 nanosheet for photocatalytic hydrogen evolution. Chemical Engineering Journal, 2021, 420, 127681.	12.7	40
32	Fe–Ni Alloy Nanoclusters Anchored on Carbon Aerogels as Highâ€Efficiency Oxygen Electrocatalysts in Rechargeable Zn–Air Batteries. Small, 2021, 17, e2102002.	10.0	38
33	Ni ^{II} Coordination to an Alâ€Based Metal–Organic Framework Made from 2â€Aminoterephthalate for Photocatalytic Overall Water Splitting. Angewandte Chemie, 2017, 129, 3082-3086.	2.0	37
34	Dynamic evolution of isolated Ru–FeP atomic interface sites for promoting the electrochemical hydrogen evolution reaction. Journal of Materials Chemistry A, 2020, 8, 22607-22612.	10.3	36
35	Hydrogen production via steam reforming of n-dodecane over NiPt alloy catalysts. Fuel, 2020, 262, 116469.	6.4	31
36	Synthesis of birnessite with adjustable electron spin magnetic moments for the degradation of tetracycline under microwave induction. Chemical Engineering Journal, 2017, 326, 329-338.	12.7	28

#	Article	IF	CITATIONS
37	Fe ultra-small particles anchored on carbon aerogels to enhance the oxygen reduction reaction in Zn-air batteries. Journal of Materials Chemistry A, 2021, 9, 6861-6871.	10.3	28
38	Singleâ€Atom Doping and Highâ€Valence State for Synergistic Enhancement of NiO Electrocatalytic Water Oxidation. Small, 2021, 17, e2102448.	10.0	28
39	Evidence of an interlayer charge transfer route in BiCu1â^'xSeO. Journal of Materials Chemistry A, 2013, 1, 12154.	10.3	27
40	Polymer precursor synthesis of TaC–SiC ultrahigh temperature ceramic nanocomposites. RSC Advances, 2016, 6, 88770-88776.	3.6	25
41	Hydroformylation of olefins catalyzed by single-atom Co(II) sites in zirconium phosphate. Journal of Catalysis, 2022, 408, 245-260.	6.2	23
42	Unraveling the Interfacial Charge Migration Pathway at the Atomic Level in a Highly Efficient Zâ€Scheme Photocatalyst. Angewandte Chemie, 2019, 131, 11451-11456.	2.0	22
43	Acid-stimulated bioassembly of high-performance quantum dots in <i>Escherichia coli</i> . Journal of Materials Chemistry A, 2019, 7, 18480-18487.	10.3	16
44	Direct Transformation of Glycerol to Propanal using Zirconium Phosphateâ€Supported Bimetallic Catalysts. ChemSusChem, 2020, 13, 4954-4966.	6.8	15
45	Sulfur-Tolerant Ni–Pt/Al ₂ O ₃ Catalyst for Steam Reforming of Jet Fuel Model Compound <i>n</i> -Dodecane. Energy & Fuels, 2020, 34, 7430-7438.	5.1	13
46	Biâ€centric view of the isostructural phase transitions in αâ€Bi ₂ Se ₃ and αâ€Bi ₂ Te ₃ . Physica Status Solidi (B): Basic Research, 2017, 254, 1700007.	1.5	11
47	Confocal depth-resolved fluorescence micro-X-ray absorption spectroscopy for the study of cultural heritage materials: a new mobile endstation at the Beijing Synchrotron Radiation Facility. Journal of Synchrotron Radiation, 2017, 24, 1000-1005.	2.4	11
48	Temperature-Dependent Structural Evolution in Au ₄₄ Ga ₅₆ Liquid Eutectic Alloy. Journal of Physical Chemistry C, 2019, 123, 25209-25219.	3.1	10
49	A facile heating cell for <i>in situ</i> transmittance andÂfluorescence X-ray absorption spectroscopy investigations. Journal of Synchrotron Radiation, 2014, 21, 165-169.	2.4	8
50	Revisiting local structural changes in GeO ₂ glass at high pressure. Journal of Physics Condensed Matter, 2017, 29, 465401.	1.8	8
51	Time-resolved XAFS measurement using quick-scanning techniques at BSRF. Journal of Synchrotron Radiation, 2017, 24, 674-678.	2.4	8
52	Structural changes in hexagonal WO3 under high pressure. Journal of Alloys and Compounds, 2019, 797, 1013-1017.	5.5	8
53	Breaking Platinum Nanoparticles to Singleâ€Atomic Pt 4 Coâ€catalysts for Enhanced Solarâ€toâ€Hydrogen Conversion. Angewandte Chemie, 2021, 133, 2571-2577.	2.0	8
54	Dynamic Restructuring of Coordinatively Unsaturated Copper Paddle Wheel Clusters to Boost Electrochemical CO ₂ Reduction to Hydrocarbons**. Angewandte Chemie, 2022, 134, .	2.0	8

#	Article	IF	CITATIONS
55	Optimal azimuthal orientation for Si(111) double-crystal monochromators to achieve the least amount of glitches in the hard X-ray region. Journal of Synchrotron Radiation, 2015, 22, 1147-1150.	2.4	7
56	Local structural changes during the disordered substitutional alloy transition in Bi2Te3 by high-pressure XAFS. Journal of Applied Physics, 2018, 124, 065901.	2.5	7
57	Local insight into the La-induced structural phase transition in multiferroic BiFeO ₃ ceramics by x-ray absorption fine structure spectroscopy. Journal of Physics Condensed Matter, 2019, 31, 085402.	1.8	7
58	A Cationic Ru(II) Complex Intercalated into Zirconium Phosphate Layers Catalyzes Selective Hydrogenation via Heterolytic Hydrogen Activation. ChemCatChem, 2021, 13, 3801-3814.	3.7	7
59	Metal Ionic Liquids Produce Metalâ€Dispersed Carbonâ€Nitrogen Networks for Efficient CO 2 Electroreduction. ChemCatChem, 2019, 11, 3166-3170.	3.7	6
60	Solvent coordination engineering for high-quality hybrid organic-inorganic perovskite films. Journal of Materials Science, 2021, 56, 9903-9913.	3.7	6
61	Superconductivity Enhancement in Fe3O4 Doped YBa2Cu3O7â^î^. Journal of Superconductivity and Novel Magnetism, 2014, 27, 693-699.	1.8	5
62	Structural phase transitions in ionic conductor Bi ₂ O ₃ by temperature dependent XPD and XAS. Journal of Physics: Conference Series, 2016, 712, 012132.	0.4	5
63	Unraveling the Low-Temperature Redox Behavior of Ultrathin Ceria Nanosheets with Exposed {110} Facets by in Situ XAFS/DRIFTS Utilizing CO as Molecule Probe. Journal of Physical Chemistry C, 2019, 123, 322-333.	3.1	4
64	Surface Ligand Tuning of Coordination Geometry and Pb 6s ² Electronic Pair Stereochemical Activity in MAPbBr ₃ Perovskite Nanoparticles: A Joint Experimental and Theoretical Insight. Journal of Physical Chemistry C, 2022, 126, 7500-7509.	3.1	4
65	Feâ€O Clusters Anchored on Nodes of Metal–Organic Frameworks for Direct Methane Oxidation. Angewandte Chemie, 2021, 133, 5875-5879.	2.0	3
66	Anharmonicity and local lattice distortion in strained Ge-dilute Si1â^'Ge alloy. Journal of Alloys and Compounds, 2015, 653, 117-121.	5.5	2
67	A method to stabilize the incident X-ray energy for anomalous diffraction measurements. Journal of Synchrotron Radiation, 2017, 24, 781-786.	2.4	1
68	Swallowâ€Nestâ€Inspired Strategy towards Ultralight Functional Multiwall arbonâ€Nanotubeâ€Based Aerogels for Supercapacitors. ChemElectroChem, 2019, 6, 1661-1667.	3.4	1
69	In situ depth-resolved synchrotron radiation X-ray spectroscopy study of radiation-induced Au deposition. Journal of Synchrotron Radiation, 2019, 26, 1940-1944.	2.4	1
70	Biâ€centric view of the isostructural phase transitions in αâ€Bi ₂ Se ₃ and αâ€Bi ₂ Te ₃ (Phys. Status Solidi B 7/2017). Physica Status Solidi (B): Basic Research, 2017, 254, 1770238.	1.5	0
71	Extracting structural information of higher coordination shells by analyzing EXAFS derivative spectrum. Physica Scripta, 2018, 93, 125701.	2.5	0
72	A new mobile grazing-incidence X-ray absorption fine spectroscopy endstation at Beijing Synchrotron Radiation Facility. Radiation Detection Technology and Methods, 0, , .	0.8	0